38

Microstructural and Mineralogical Characterization of Clay Stabilized Using Calcium-Based Stabilizers

Pranshoo Solanki[1] and Musharraf Zaman[2]
[1]*Illinois State University*
[2]*University of Oklahoma*
USA

1. Introduction

The properties of clays can be significantly improved by treating with calcium-based stabilizers (or additives) such as hydrated lime (or lime), Portland cement, cement kiln dust (CKD), and class C fly ash (CFA). In the presence of water, the calcium ions released from these stabilizers reduce the thickness of double diffused layer through cation-exchange and flocculation-agglomeration reactions. This is primarily responsible for improvement in workability through reduction of adsorbed water and decrease in plasticity index. In long-term, pozzolanic reactions occur between the calcium ions of the stabilizer and the silica and alumina of the clay minerals resulting in the formation of cementitious products such as calcium-silicate-hydrates (C-S-H), calcium-aluminate-hydrates (C-A-H), and calcium-aluminum-silicate-hydrates (C-A-S-H). The reaction may be written as:

$$Ca(OH)_2 \text{ (ionization of lime)} \rightarrow Ca^{2+} + 2(OH)^- \quad (1)$$

$$Ca^{2+} + OH^- + SiO_2 \text{ (soluble clay silica)} \rightarrow \text{calcium-silicate-hydrate} \quad (2)$$

$$Ca^{2+} + OH^- + Al_2O_3 \text{ (soluble clay alumina)} \rightarrow \text{calcium-aluminate-hydrate} \quad (3)$$

The hyphens indicate that the composition is indefinite. The specific composition is defined by pH level, solubility of silica and alumina, clay mineralogy, and curing conditions among other reasons. C-S-H, formed by the hydration of C_3S, is also commonly known as tobermorite gel. The tobermorite gel is poorly crystalline, with only a few broad, weak bands in its X-ray diffraction pattern (Mohamed, 2002). C-A-H is formed as platelets with hexagonal symmetry. The morphology of both C-A-H and C-A-S-H resembles that of tobermorite gel. In the presence of calcium sulfate, an additional product of hydration, known as ettringite ($Ca_6[Al(OH)_6]_2.(SO_4)_3.26H_2O$) is formed (Eq. 4). Ettringite mineral consists of a prismatic crystal and a hexagonal cross section.

$$6Ca^{2+} + 2Al(OH)_4^- + 4OH^- + 3SO_4^{2-} + 26H_2O \rightarrow Ca_6[Al(OH)_6]_2.(SO_4)_3.26H_2O \quad (4)$$

The formation of aforementioned cementitious products in the soil-stabilizer matrix are responsible for increase in the internal friction and shear strength of the stabilized soil.

However, the efficacy of stabilization depends on the soil mineralogy, type and amount of stabilizer, and curing conditions (e.g., time, temperature, moisture). Although several researchers studied the improvement in engineering properties of stabilized soil at macro level (e.g, shear strength, unconfined compressive strength, swell behavior), very few studies discussed the changes in soil-stabilizer matrix at micro level. Consequently, the primary objective of this study is to examine the changes in microstructure and mineralogy of soil due to stabilization with calcium-based stabilizer. Additionally, at macro level the modulus of elasticity values are evaluated for both raw and stabilized specimens and correlated with microstructural and mineralogical characteristics.

2. Literature review

Several investigations were carried out to study the changes in the microstructural and mineralogical characteristics of stabilized soils. Rajasekaran et al. (1995) studied the influence of sodium hydroxide on the fabric of lime treated marine clays using scanning electron microscopy (SEM) technique. It was found that lime stabilization is very effective for marine clays. Adding sodium hydroxide additive resulted in better formation of pozzolanic compounds. Formation of cementitious compounds such as C-A-H and C-S-H due to the soil-lime reactions were observed in all lime treated soils which were further confirmed by using X-Ray Diffraction (XRD) technique. The study conducted by using SEM indicated that there is an overall improvement in the structure of the soil system resulting in a porous system and aggregate formation. However, this study was limited to only lime-stabilization.

In another study, Lav and Lav (2000) investigated the effects of cement- and lime-stabilization on class F fly ash in terms of change in chemical composition, crystalline structures, and hydration products. The unconfined compressive strength (UCS) of samples was also evaluated over time to observe the effect of stabilization. Cement- and lime-stabilized fly ash produced similar hydration products. None of these produced was recognizable by XRD except weak calcium hydroxide (CH) and calcium carbonate due to carbonation. The improvement in microstructure was found initiating from fly ash particles serving as nucleation centers for hydration or pozzolanic reaction products. The increasing strength gain was attributed to growth of hydrates in the voids between the particles. However, no attempt was made to study the influence of aforementioned additives on soil.

Ghosh and Subbarao (2001) studied the physicochemical and microstructural developments of fly ash-lime- and fly ash-lime-gypsum-stabilized materials. Different analytical techniques namely, XRD, differential thermal analysis, SEM, and Energy Dispersive Spectroscopy (EDS) were used for studying the microstructure. The SEM micrographs revealed evidence of the development of a compact matrix after three months of curing time and a densified compact network of pozzolanic reaction products of fly ash-lime-gypsum with the increase in the curing period to ten months. The XRD analysis results indicated appearance of new peaks of low intensity in the modified fly ash specimens. Some of these peaks were not recognized as part of any new crystalline phases. Similar to previous study, this study was limited to fly ash-lime mixtures and no attempt was made to study the influence of these additives on soil.

In a laboratory study, Al-Rawas (2002) investigated the microfabric and mineralogical aspects of the expansive soil using cement by-pass dust (CBPD), copper slag, slag-cement,

and ground granulated blast furnace slag (GGBFS). The highest swell potential of untreated soil was explained by the presence of the highest percentage of sodium smectite clay mineral along with palygorskite and illite in soil. The fabric of the untreated soil was found composed of dense clay matrices with no appearance of aggregations and increasing amount of pore spaces. However, stabilization resulted in the formation of aggregations and few connectors. It was found that higher amount of sodium ions and lower amount of calcium ions promotes swelling and vice versa. Further, the XRD results showed a general reduction in all the clay minerals' peak intensities particularly in the case of CBPD treated samples. This study addressed most of the properties that will be evaluated in the present study. However, it was carried out on predominantly silty soil stabilized with non-traditional additives. It is also important to note that the mineralogical and textural characteristics of fat clay used in the present study are different than silty soil. Also, non-traditional additives are not commonly available and are expensive. This makes it necessary to investigate locally available additives such as lime, fly ash, and CKD.

Stutzman (2004) studied the bulk and surface phase composition of hydraulic cement using SEM in conjunction with XRD. Direct imaging of hydraulic cements obtained through SEM yielded complete picture of both bulk and surface phase compositions. Mass percent and volume percent were calculated by analyzing resulting composite image from SEM. A good agreement was found between mass percentages obtained by SEM imaging and percentages based upon quantitative XRD. The finer grained phases (e.g., gypsum, tricalcium aluminate, and ferrite) showed much higher surface areas per unit mass than the coarser-grained phases such as alite and belite. But no attempt was made to compare the microstructures of stabilized soils.

In another laboratory study, Kolias et al. (2005) investigated the effectiveness of using high calcium fly ash and cement in stabilizing lean and fat clays. Strength tests in compression, indirect tension, and flexure modes were conducted on stabilized samples. Additionally, thermogravimetric-single differential thermal analysis (TG-SDTA) and XRD tests were conducted on selected samples to study the hydraulic compounds. The study showed the potential benefit of stabilizing clays with high calcium fly ash. However, it was found that the effectiveness of stabilization is dependent on the type of soil, the amount of stabilizer and the curing time. The study of formation of hydraulic products showed that a significant amount of tobermorite gel is formed due to stabilization leading to a denser and more stable structure of the samples. The mechanical properties such as strength and modulus of elasticity showed considerable enhancement due to stabilization. This study, however, did not examine the microstructure of lime- and CKD-stabilized soils.

Horpibulsuk et al. (2010) analyzed the strength development in cement-stabilized silty clay based on microstructural considerations. A qualitative and quantitative study was conducted on the microstructure using a SEM, mercury intrusion pore size distribution measurements, and thermal gravity analysis. A total of three zones of improvement namely, active, inert, and deterioration zones, were observed. The active zone was found to be most effective for stabilization where the cementitious products increased with cement content and filled the pore space. In the inert zone, both pore size distribution and cementitious products change insignificantly with increasing cement. In deterioration zone, the water is not adequate for hydration because of the excess of cement input. It was found that in short stabilization period, the volume of large pores (> 0.1 μm) increases because of input of

coarser particles while the volume of small pores (< 0.1 μm) decreases because of the solidification of the hydrated cement. With time, the large pores are filled with the cementitious products; thus, the small pore volume increases, and the total pore volume decreases resulting in the development of strength with time. This study, however, was limited to only cement and no attempt was made to compare the microstructure of soil stabilized with other additives.

In a recent study, Chaunsali and Peethamparan (2011) characterized a nontraditional binding material containing cement kiln dust (CKD) and ground GGBFS. The CKD used in this study contained low free lime and high sulfate and alkali content, and proved effective in accelerating the hydration of GGBFS. The strength rate development was found to be dependent on the curing conditions but eventually all the samples achieved similar compressive strengths independent of the curing conditions. The microstructural and mineralogical examinations showed that the strength development was mainly due to the formation of C-S-H. Additionally, aluminum and magnesium incorporated C-S-H phases were also identified in CKD-GGBFS blends. The formation of ettringite appeared as a contributing factor in the development of early age strength in CKD-GGBFS binder.

It is clear from the aforementioned literature review that there is a lack of detailed comparative studies on microstructure and mineralogy of expansive soils stabilized with various stabilizers. Therefore, there was a need to undertake a detailed investigation to fully characterize the microstructure and mineralogy of soil stabilized with locally available additives.

3. Materials and sources

In the present study, one fat clay and three cementitious additives are used. This section describes the fundamental properties including grain size distribution, index properties and chemical compositions of the soils and additives.

3.1 Native soils

The soil used in this study is Carnasaw series soil. According to the Unified Soil Classification System (USCS), Carnasaw series soil is classified as fat clay (CH) with an average liquid limit of approximately 58% and a plasticity index (PI) of 29 in accordance with ASTM D 4318 test method. The gradation tests revealed percent passing No. 200 sieve (< 0.075 mm) and clay content (< 0.002 mm) as 94% and 48%, respectively. A summary of the physical and chemical properties of the selected soil is presented in Table 1.

3.2 Cementitious additives

As noted earlier, three different cementitious additives, namely, hydrated lime, CFA, and CKD were used. Hydrated lime was supplied by the Texas Lime Company, Cleburne, Texas. It is a dry powder manufactured by treating quicklime (calcium oxide) with sufficient water to satisfy its chemical affinity with water, thereby converting the oxides to hydroxides. CFA from Lafarge North America (Tulsa, Oklahoma) was brought in well-sealed plastic buckets. It was produced in a coal-fired electric utility plant, American Electric Power (AEP), located in Muskogee, Oklahoma. CKD used was provided by Lafarge North America located in Tulsa, Oklahoma. It is an industrial waste collected during the

production of Portland cement. The physical and chemical properties of the stabilizing agents are presented in Table 1. The X-Ray Fluorescence (XRF) analysis was conducted using a Panalytical 2403 spectrometer on specimens obtained by using fused bead preparation method. The fused bead preparation technique consists of dissolving the specimen in a solvent called a flux at high temperature (>1000°C) in a platinum crucible and to cast it in a casting-dish. It is evident from Table 1 that the calcium oxide content in hydrated lime is 68.6%. This can be explained using the stoichiometry of the chemical reaction taking place during the specimen preparation for XRD.

$$\underset{(74)=40x1+16x2+1x2}{Ca(OH)_2} \rightarrow \underset{(56)=40x1+16x1}{CaO} + \underset{(18)=1x2+16x1}{H_2O} \quad (5)$$

Using above chemical equation, it can be shown that 95.9% of $Ca(OH)_2$ (reactant) will produce approximately 72% of CaO (product). Further, the free lime content (i.e., any lime not bound up in glassy phase compounds such as tricalcium silicate and tricalcium aluminate) was determined in accordance with ASTM C 114 (Alternate Test Method B, ammonium acetate titration). Although CFA is having a very low lime content (0.2%), specimens stabilized with CFA showed enhancement in strength and modulus values as will be discussed later in this chapter. It is speculated that during the reaction process some lime is liberated from the bound state which takes part in the cementitious reactions and thus, producing increase in strength and modulus values.

Chemical compound/Property	Percentage by weight, (%)			
	Lime	CFA	CKD	Soil
Silica (SiO_2)[a]	0.6	37.7	14.1	63.4
Alumina (Al_2O_3)[a]	0.4	17.3	3.1	21.5
Ferric oxide (Fe_2O_3)[a]	0.3	5.8	1.4	9.1
Calcium oxide (CaO)[a]	68.6	24.4	47	0.1
Calcium hydroxide ($Ca(OH)_2$)[a]	95.9**	…	…	…
Magnesium oxide (MgO)[a]	0.7	5.1	1.7	1.2
Sulfur trioxide (SO_3)[a]	0.1	1.2	4.4	0
Alkali content ($Na_2O + K_2O$)[a]	0.1	2.2	1.7	3.0
Loss on ignition[b]	31.8*	1.2	27	…
Free lime[b]	46.1	0.2	6.7	…
Percentage passing No. 325[c]	98.4	85.8	94.2	87.2
pH (pure material)[d]	12.58	11.83	12.55	4.17
Specific surface area (m^2/gm)[e]	17.0	6.0	12.0	118.5
28-day UCS (kPa)	…	708	17	207

[a]X-ray Fluorescence analysis; [b]ASTM C 114; [c]ASTM C 430; [d]ASTM D 6276; [e]Ethylene glycol monoethyl ether method (Cerato and Lutenegger 2001); UCS: Unconfined compressive strength;
*Ca(OH)2 decomposes at 512oC; **Before ignition

Table 1. Chemical and physical properties of soil and additives

4. Factors affecting cementitious stabilization

The effectiveness of cementitious stabilization depends on properties of both soil and additive (AFJMAN, 1994, Al-Rawas et al., 2002, Parsons et al., 2004, Evangelos, 2006). A description of the pertinent factors intrinsic to the soils and additives which influence the efficiency of cementitious stabilization is presented herein.

4.1 Soil properties

4.1.1 Gradation and plasticity index

Several researchers (e.g., Diamond and Kinter, 1964; Haston and Wohlgemuth, 1985; Prusinski and Bhattacharja, 1999; Little, 2000; Qubain et al., 2000; Kim and Siddiki, 2004; Mallela et al., 2004; Puppala et al., 2006; Consoli et al., 2009) recommended use of lime with fine-grained soils. However, CFA (see e.g., McManis and Arman, 1989; Chang, 1995; Misra, 1998; Zia and Fox, 2000; Puppala et al., 2003; Bin-Shafique et al., 2004; Phanikumar and Sharma, 2004; Nalbantoglu, 2004; Camargo et al., 2009; Li et al., 2009) and CKD (e.g., McCoy and Kriner, 1971; Baghdadi and Rahman, 1990; Zaman et al., 1992; Sayah, 1993; Miller and Azad, 2000; Miller and Zaman, 2000; Parsons and Kneebone, 2004; Sreekrishnavilasam et al., 2007; Peethamparan et al., 2008; Gomez, 2009) is used successfully with both fine- and coarse-grained soils. Lower effectiveness of lime with coarse-grained soil can be attributed to scarcity of pozzolana (silicious and aluminacious material) in coarse-grained soils which is required for pozzolanic (or cementitious) reactions. Little (2000) and Mallela et al. (2004) recommend a soil with a minimum clay content (< 0.002 mm) of 10% and a plasticity index of 10 for lime-stabilization. In this study, Carnasaw series soil fulfils this requirement with a clay content of 48%. Also, mineralogical analyses conducted using XRF revealed that the soil used in this study is having high (85%) amount of pozzolana, as presented in Table 1.

4.1.2 Cation exchange capacity

Cation Exchange Capacity (CEC) is the quantity of exchangeable cations required to balance the charge deficiency on the surface of the clay particles (Mitchell, 1993). During ion-exchange reaction of soil with cementitious additive, cation of soil (e.g., Na^+, K^+) is replaced by cation of additive (Ca^{2+}) and the thickness of double diffused layer is reduced. Hence, the replacement of cations results in an increase in workability and strength of soil-additive mixture. The rate of exchange depends on clay type, solution concentrations and temperature (Gomez, 2009). In soil stabilization studies, CEC values have been used to a limited extent to explain the effectiveness of soil stabilization (Nalbantoglu and Tuncer, 2001; Al-Rawas et al., 2002; Nalbantoglu, 2004; Gomez, 2009).

In this study, CEC was measured by sodium acetate method in accordance with the EPA 9081 test method (Chapman, 1965). As evident from Table 1, Carnasaw soil showed CEC value of 5.2 meq/100 gm.

4.1.3 Sulfate content

Primary "sulfate-induced heaving" problems arise when natural sulfate rich soils are stabilized with calcium-based additives (Puppala et al., 2004), also known as "sulfate attack." This heave is known to severely affect the performance of pavements, and other

geotechnical structures built on sulfate rich soils stabilized with calcium-based additive (Hunter, 1988; Mitchell and Dermatas, 1990; Petry and Little, 1992; Rajendran and Lytton, 1997; Rollings et al., 1999; Puppala et al., 2004). According to current understanding, "low to moderate" and high sulfate soils are those with sulfate less than 2,000 ppm and more than 2,000 ppm, respectively (Kota et al., 1996; Mitchell and Dermatas, 1990; Puppala et al., 2002; Rao and Shivananda, 2005). In this study, soluble sulfate content in the soil was measured using the Oklahoma Department of Transportation procedure for determining soluble sulfate content: OHD L-49 (ODOT, 2006). No detectable sulfate content (< 200 ppm) was found in the soil used in this study.

4.1.4 Specific surface area

Surface phenomena have an important influence on the behavior of fine-grained soils; they affect many physical and chemical properties (Cerato and Lutenegger, 2002). The specific surface area (SSA), refers to the area per unit mass of soil, may be a dominant factor in controlling the fundamental behavior of many fine-grained soils (Gomez, 2009). The mineralogy of fine-grained soils is the dominant factor in determining the effect of SSA. For this study, only total SSA measurement was conducted using the polar liquid Ethylene Glycol Monoethyl Ether (EGME) method (Cerato and Lutenegger, 2002) and results are presented in Table 1. The Carnasaw series soil showed a SSA value of 118.5 m^2/gm.

4.2 Additive properties

4.2.1 Free-lime content

In calcium-based stabilizers (e.g., Portland cement, CFA, CKD) most of the lime (CaO) is bound up in compounds such as tricalcium silicate and tricalcium aluminate. The unreacted lime that is not combined in any of these compounds is called free-lime, which is expected to play a major role in stabilization (Collins and Emery, 1983; Misra, 1998; Zaman et al., 1998; Ferguson and Levorson, 1999; Miller and Azad, 2000; Miller and Zaman, 2000; Sezer et al., 2006; Khoury and Zaman, 2007; Peethamparan and Olek, 2008). Free-lime content was determined by conducting titration in accordance with ASTM C 114 alternative test method B and results are presented in Table 1. It is clear that lime is having the highest free-lime content of 46.7% followed by 6.7% for CKD and 0.2% for CFA.

4.2.2 Specific surface area

The specific surface area (SSA) of additives, as measured by using the ethylene glycol monoethyl ether (EGME) method (Cerato and Lutenegger, 2002), were 17.0, 6.0, and 12.0 m^2/gm, respectively, for lime, CFA and CKD. It can be seen that lime and CFA had the highest and the lowest SSA values, respectively. A higher SSA indicates more reactivity of additive (Nalbantoglu and Tuncer, 2001; Sreekrishnavilasam et al., 2007).

4.2.3 Loss on ignition

A higher loss on ignition (LOI) value indicates high carbonates for CFA/CKD and high hydroxides for lime. Some researchers reported that high LOI indicates low free-lime content for CKDs, making CKDs less reactive, and therefore lower improvements (Bhatty et

al., 1996; Miller and Azad, 2000). In the laboratory, LOI was evaluated by igniting additive inside a muffle furnace at a temperature of 950°C (1742°F) in accordance with ASTM C 114 test method for hydraulic cements. As evident from results presented in Table 1, lime and CFA produced highest and lowest LOI values of 31.8% and 1.2%, respectively. On the other hand, approximately 27% of CKD is lost on ignition.

4.2.4 Percent passing No. 325 sieve

Several researchers noticed increased reactivity of additive with increase in amount of additive passing No. 325 (45 μm) sieve (NCHRP, 1976; Bhatty et al., 1996; Zaman et al., 1998; Zheng and Qin, 2003; Khoury, 2005). The percentage of passing No. 325 sieve for lime, CFA and CKD determined in accordance with ASTM C 430 test method are 98.4, 85.8 and 94.2, respectively. It is clear that lime is finest among all the additives used in this study.

4.2.5 pH and pH response

The elevated pH level of soil-lime mixture is important because it provides an adequate alkaline environment for ion-exchange reactions (Little, 2000). In the laboratory, pH is determined using the method recommended by ASTM D 6276 for lime-stabilization, which involves mixing the solids with de-ionized (DI) water, periodically shaking samples, and then testing with a pH meter after 1 h. The procedure specifies that enough lime must be added to a soil-water system to maintain a pH of 12.4 after 1 h. This ensures that adequate lime is provided to sustain the saturation during the 1-h period (Prusinski and Bhattacharja, 1999).

Additive Content (%)	Lime		Additive Content (%)	CFA		Additive Content (%)	CKD	
	pH value	% Increase[a]		pH value	% Increase[a]		pH value	% Increase[a]
0	4.17	---	0	4.17	---	0	4.17	---
1	9.22	121.1	2.5	5.19	24.5	2.5	7.05	69.1
3	12.23	193.3	5	5.93	42.2	5	8.8	111.0
5	**12.54**	**200.7**	7.5	6.55	57.1	7.5	10.11	142.4
6	12.55	201.0	10	7.79	86.8	10	10.88	160.9
7	12.55	201.0	12.5	8.32	99.5	12.5	11.28	170.5
9	12.57	201.4	15	8.86	112.5	15	11.62	178.7
100	12.58	201.7	17.5	9.47	127.1	17.5	11.98	187.3
			100	4.17	---	100	4.17	---

[a]Increase in pH w.r.t. pH value of raw soil; Bold values represent minimum additive content providing asymptotic behavior (< 1% increase)

Table 2. Variation of pH values with soil and additive type

Several researchers (e.g., Haston and Wohlgemuth, 1985; Prusinski and Bhattacharja, 1999; IRC, 2000; Little, 2000; Qubain et al., 2000; Mallela et al., 2004; Puppala et al., 2006; Consoli et al., 2009) used pH values on soil-lime mixture as an indicator of reactivity of lime. However, only limited studies (see e.g., Miller and Azad, 2000; Parsons et al., 2004; Peethamparan and Olek, 2008; Gomez, 2009) evaluated pH response of soil-CFA or soil-CKD mixtures. Hence,

the pH values of soil-additive mixtures were determined to investigate whether pH would reflect the effectiveness of soil stabilization with lime, CFA or CKD.

The pH results of raw soil, raw additive and soil-additive mixtures are presented in Table 2 and are used as the primary guide for determining the amount of additive required to stabilize each soil. It is clear that Carnasaw soil is acidic with a pH value approximately 4.17. Also, it was found that raw lime, CFA and CKD had a pH value of 12.58, 11.83 and 12.55, respectively. The pH values of raw CFA and CKD are consistent with the results reported by other researchers (e.g., Miller and Azad, 2000; Sear, 2001; Parsons et al., 2004; Peethamparan and Olek, 2008; Gomez, 2009). The pH trend of raw additives is similar to the trend of available free-lime content in additive, as shown in Table 1.

For all the soil-additive mixtures, pH values increase with the increase in the percentage of additive and show an asymptotic behavior after a certain percentage. In the current study, an increase of less than 1% in pH with respect to raw soil is assumed as starting point of the asymptotic behavior. As evident from Table 2, pH values started showing an asymptotic behavior with 5% lime. Additionally, soil never attained an asymptotic behavior with CFA and CKD contents up to 17.5%. This can be attributed to the acidic behavior of Carnasaw soil which requires higher amounts of moderately basic CFA and CKD for neutralization. Based on the aforementioned observations, it was decided to select 9% of lime and 15% of CFA and CKD for laboratory performance evaluation.

5. Experimental methodology

5.1 Specimen preparation

In this study, a total of 16 specimens were prepared for evaluating modulus of elasticity. The procedure consists of adding a specific amount of additive to the raw soil desired. The amount of additive (9% for lime and 15% for CFA and CKD) was added based on the dry weight of the soil. The additive and soil were mixed manually for uniformity. After the blending process, a desired amount of water was added based on the optimum moisture content (OMC). The mixture was then compacted in a mold having a diameter of 101.6 mm and a height of 203.2 mm to reach a dry density of between 95%-100% of the maximum dry unit weight (MUW). After compaction, specimens were cured at a temperature of 23.0 ± 1.7^{o}C and a relative humidity of approximately 96% for 28 days. A total of four replicates were prepared for each additive type and tested for modulus of elasticity in accordance with ASTM D 1633 test method.

5.2 Modulus of elasticity

As noted earlier, modulus of elasticity test was conducted in accordance with the ASTM D 1633 test method. Specimens were loaded in a MTS frame at a constant strain rate of 0.63% (of sample height) per minute, which is equivalent to 1.27 mm (0.05 in.) per minute for the specimen configuration used here. Deformation values were recorded during the test using LVDTs fixed to opposite sides of and equidistant from piston rod with a maximum stroke length of ±12.7 mm (±0.5 in). The load values were obtained from a load cell having a capacity of 22.7 kN (5,000 lb). Each specimen was subjected to two unloading-reloading cycles. Straight lines were drawn through the first two unloading-reloading curves (secant

modulus) and the average slope of these lines is the modulus of elasticity of the stabilized clay specimen.

5.3 Mineralogical studies

To facilitate the macro-behavior comparison and explanation, the mineralogical study techniques namely SEM and EDS were employed to qualitatively identify the micro-structural developments in the matrix of the stabilized soil specimens. The SEM technique was employed using a JEOL JSM 880 microscope to qualitatively identify the micro-structural developments in the matrix of the stabilized soil specimens. After the modulus of elasticity test, specimens were broken and mix was air-dried for approximately two days. Three representative tiny pieces were mounted on stubs (1 cm, i.e., 0.4 in. wide discs having a pin-mount on the base of the disc). The samples were not electrically conductive; therefore, they were initially coated by Iridium to maintain conductivity. The quality of images was not satisfactory, so it was decided to use gold-palladium alloy for the process instead of Iridium coating. Hence, pieces were coated with a thin layer (≈ 5 nm) of an alloy of gold-palladium by sputter coating technique to provide surface conductivity. A JEOL JSM 880 scanning electron microscope operating at 15 kV was used to visually observe the coated specimens. The JEOL JSM 880 was fitted with an energy-dispersive X-ray spectrometer (EDS). The EDS was used to analyze chemical compositions of the specimen. In this technique, electrons are bombarded in the area of desired elemental composition; the elements present will emit characteristic X-rays, which are then recorded on a detector. The micrographs were taken using EDS2000 software. It must be noted that SEM study allows only a tiny area of raw and stabilized specimen to be examined (unlike engineering laboratory specimens). However, it is believed to be representative of the reaction process of stabilized specimens. Figure 1 (a) shows a photographic view of JEOL JSM 880 setup along with Hummer VI triode sputter coater.

(a) (b)

Fig. 1. (a) JEOL JSM 880 setup for SEM, Hummer VI triode sputter coater with sample (corner picture), and (b) Rigaku D/Max X-ray diffractometer

The XRD tests were performed on raw soil and stabilized specimens. Two-day air dried mix was pulverized with a mortar and pestle, sieved through a U.S. standard No. 325 sieve (45 μm). Then, the powder finer than 45 μm was collected, mixed with methanol, and placed on

a specimen holder. The holder containing specimen was oven dried for approximately 15 minutes prior to testing. This holder was then mounted on a Rigaku D/Max X-ray diffractometer for analysis. This diffractometer is equipped with bragg-brentano parafocusing geometry, a diffracted beam monochromator, and a conventional copper target X-ray tube set to 40 kV and 30 mA. The measurements were performed from 4^o to 70^o (2θ range), with 0.05^o step size and 5 seconds count (dwell time) at each step. Data obtained by the diffractometer were analyzed with Jade 3.1, an X-ray powder diffraction analytical software, developed by Materials Data, Inc. (Jade, 1999). Generated diffractograms (using the peaks versus 2θ and d-spacing) were used to determine the presence of minerals. Figure 1 (b) shows a photographic view of Rigaku D/Max X-ray diffractometer.

6. Presentation and discussion of modulus of elasticity test results

The variation of modulus of elasticity values with the additive content is shown in Figure 2. It is clear from Figure 2 that the modulus of elasticity of stabilized specimens is influenced by the type of additive. For example, an increase of approximately 99%, 94% and 193% in modulus of elasticity values was observed for 9% lime-, 15% CFA- and 15% CKD-stabilized specimens, respectively. Overall, 15% CKD-stabilized specimens showed the highest improvement.

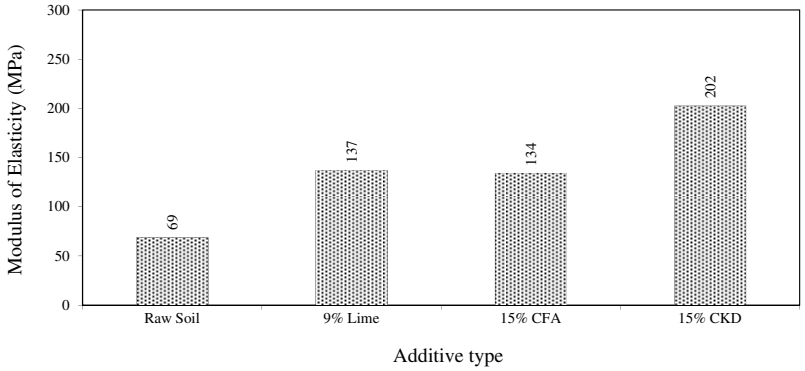

Fig. 2. Variation of modulus of elasticity values with additive type

Attempts were made to observe the effect of additive properties, namely, free-lime content, alkali content, loss on ignition, specific surface area (SSA), pH, and passing No. 325 sieve, on the modulus of elasticity. The effect of these additive properties on normalized modulus of elasticity (modulus of elasticity value/percent additive) is depicted in Figure 3. Here, it is clear that the normalized modulus of elasticity value increases with the free-lime content. The Carnasaw soil specimens exhibited an increase of approximately 13 to 15 as the free-lime content increased from 6.7% (CKD) to 46.1% (lime). A decrease in normalized modulus of elasticity values with alkali content can be observed; however, increase in normalized modulus of elasticity values with loss on ignition was observed. This trend is contrary to the behavior reported by other researchers for different type of CKDs (e.g., Bhatty et al., 1996; Miller and Azad, 2000; Peethamparan and Olek, 2008). For example, Bhatty et al. (1996) reported that CKDs

containing less than 6% alkalis and low LOI values are reactive and produces higher strength. This difference in behavior could be attributed to other factors such as free-lime content that might have influenced in enhancing the effectiveness of the additives. Although CFA had higher alkali content and lower LOI than lime, it also had lower free-lime content (0.2% for CFA versus 46.1% for lime).

Further, it is clear from Figure 3 that percent passing No. 325 sieve influences the Mr values. An increase in percent passing No. 325 sieve from 85.8% (CFA) to 98.4% (lime) increased the normalized modulus of elasticity values from 9 to 15 for P-soil. This can be attributed to increase in fine contents in the soil and thus increased surface area for pozzolanic reactivity. Normalized modulus of elasticity values versus SSA of additive are shown in Figure 3. It is clear that normalized modulus of elasticity increases with increase in SSA. The fact that the additive particles have a larger surface to interact with the soil can explain this behavior. Larger SSA values imply more available surface for soil-additive interaction resulting in more cementitious products and thus higher gain in modulus values. The pH value of additive also plays an important role in enhancing the modulus values, as evident from Figure 3. An increase in normalized modulus values with pH can be observed from Figure 3. Lime-stabilized specimens having highest pH value of 12.58 produced the highest modulus value followed by CKD- (pH = 12.55) and CFA- (pH = 11.83) stabilized specimens. As discussed earlier, high pH value causes silica from the clay minerals to dissolve and, in combination with Ca^{2+} form calcium silicate and calcium aluminate hydrate (Eades, 1962; Diamond and Kinter, 1964).

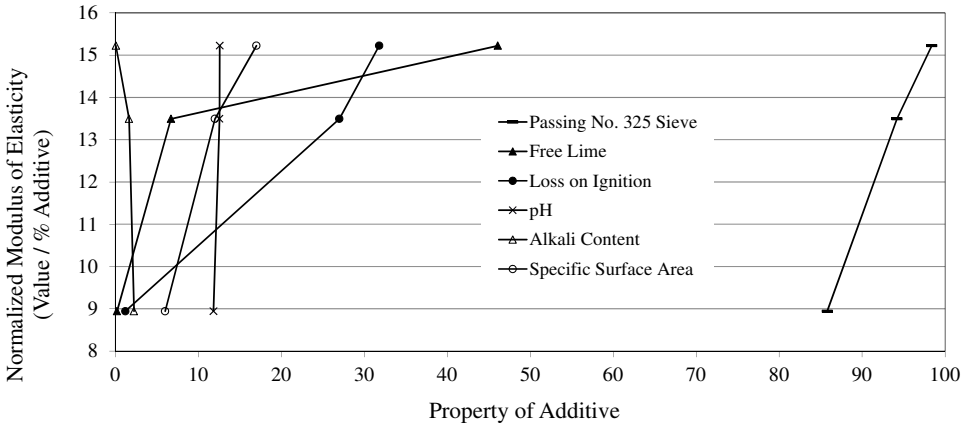

Fig. 3. Variation of normalized modulus of elasticity values with different properties of additives

7. Microstructure and mineralogical characteristics

As noted earlier, mineralogical studies namely SEM and EDS were conducted on all the raw soils, raw additives powder, raw additives paste and 28-day cured stabilized Carnasaw soil specimens to study the influence of stabilization on microstructure and mineralogical characteristics.

7.1 Raw soil and additives powder

Figure 4 (a) shows the SEM micrographs of raw Carnasaw soil sample at high magnification (10,000 times). It is clear that the raw soil has a discontinuous structure, where the voids are more visible because of the absence of hydration products. The EDS results showed majority of silicon (Si) and aluminium (Al) minerals and trace amounts of potassium (K), iron (Fe) and sodium (Na) minerals in the raw soil. The raw additives used in this study were also studied using the SEM/EDS methods. Figures 4 (b), (c) and (d) show SEM/EDS of raw lime, CFA and CKD powder, respectively. As evident from Figure 4 (b), raw lime is an amorphous powder consisting mainly of calcium (Ca) compounds. This is in agreement with the XRF results reported in Table 1. On the other hand, CFA and CKD are more complex compounds. The EDS results indicated presence of Ca, Al, Si, Fe, sulphur (S), phosphorous (P), titanium (Ti), and magnesium (Mg) minerals in CFA. Whereas EDS results of CKD indicated presence of Ca, Si, Mg, S, and K minerals.

The SEM micrographs of raw CFA showed that CFA is composed of different size spherical particles (or cenosphere); however, CKD micrographs showed particles with poorly defined shapes. The gold (Au) and palladium (Pd) peaks that appeared in all EDS spectra is due to the gold-palladium sputter coating used on SEM samples for making them electrically conductive.

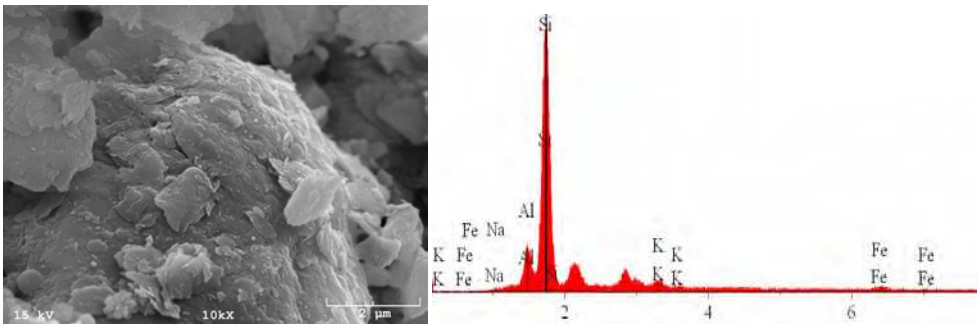

(a)

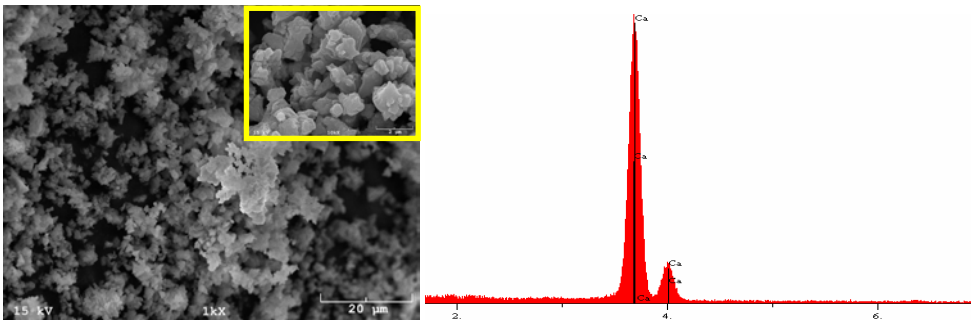

(b)

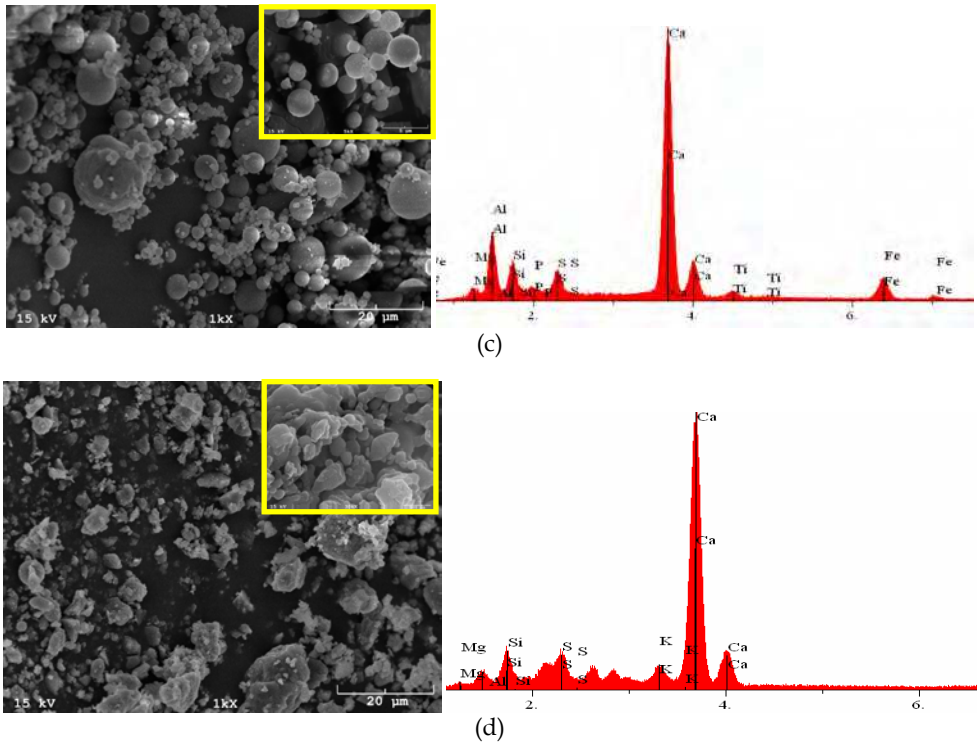

Fig. 4. SEM/EDS of (a) Raw Soil (b) Lime, (c) CFA, and (d) CKD Powder

7.2 Raw additives paste

The representative SEM micrographs of raw lime, CFA and CKD paste samples that had been subjected to 28 day curing and air dried for approximately two days are presented in Figures 5 (a) through (c). Figures 4 (b) and 5 (a) show very similar microstructure and EDS results, as expected in lime due to its negligible self-cementing properties. At a higher magnification (x 30,000 times), a flower-like structure of calcium hydroxide crystals is evident. Figure 5 (b) shows the SEM micrographs of raw CFA paste at a magnification level of 5,000. Overall, the microstructure of CFA paste had a relatively finer matrix with cenospheres covered with cementitious products. Based on EDS at different locations, the microstructure consisted of C-A-S-H like crystals with variable amounts of Al, Si, and Mg incorporated phases and traces of Fe and Ti as impurities. The Ca/Si ratio was observed to be approximately 2. The microstructure of CKD paste (Figure 5 (c)) is clearly denser and compact as compared to the microstructure of raw CKD powder (Figure 4 (d)). At a higher magnification (x 20,000 times), C-S-H gel is evident. The microstructure in combination with EDS spectrum gave an indication of the formation of C-S-H phases with Ca/Si ratio of less than 1. Please note that the EDS spectrum presented in this study were collected from a fractured surface of specimen and not from the polished smooth surface of specimen. Hence, the heights of the peaks were used as a qualitative measure rather than a quantitative measure of different crystal phases.

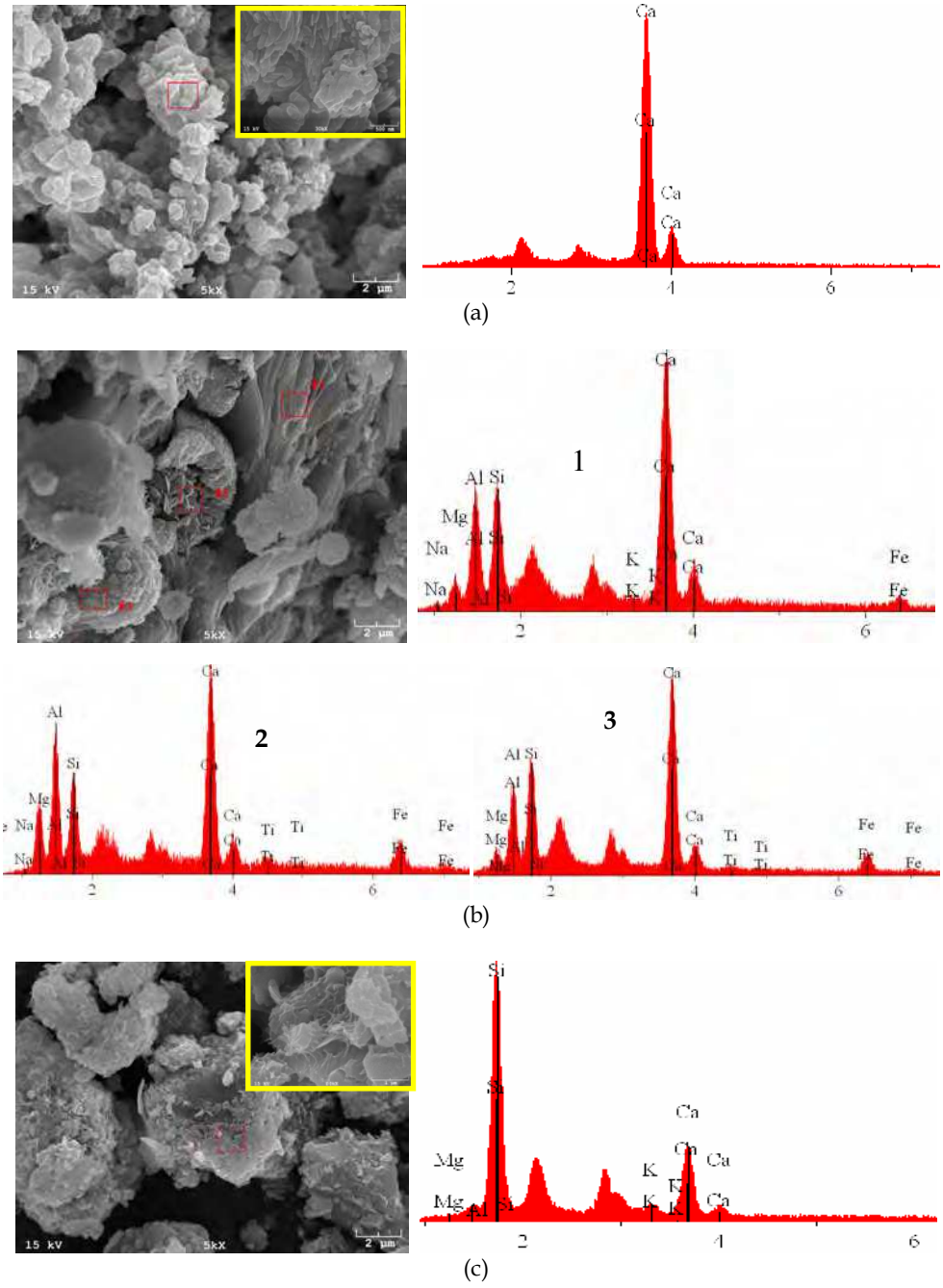

Fig. 5. SEM/EDS of (a) Lime, (b) CFA, and (c) CKD Pastes

7.3 Carnasaw soil with 9% lime

To study the microstructure of 9% lime-stabilized Carnasaw soil specimens, 28-day modulus of elasticity tested specimens were examined using SEM micrographs. Figure 6 (a) shows the microstructure at a magnification level of 10,000, which when compared with the raw soil micrograph of Figure 4 (a) shows marked change in morphology. From Figure 6 (a), it is clear that the raw soil structure has transformed from a particle based form to a more integrated composition due to cementitious reactions. At a higher magnification (x 25,000 times), the cementing phases could clearly be seen. Further, EDS pattern was used as a basis to monitor the changes occurring in the chemical composition at selected locations within the Carnasaw soil after stabilization with 9% lime. As evident from Figure 6 (a), analysis on the cementing phases showed presence of Ca and Si with high Ca/Si ratio (>7), which is an indication of the presence of C-S-H ($xCaO.ySiO_2.zH_2O$).The other two peaks not marked in Figure 6 (a) belong to Au-Pd coating The cementing phases, due to gradual crystallization of the new secondary minerals, caused an increase in the modulus of elasticity of the stabilized soil, as discussed in Section 6. Similar observations were reported by other researchers (see e.g., Locat et al., 1996; Ghosh and Subbarao, 2001; Nalbantoglu, 2006; Kavak and Akyarh, 2007). Figure 6 (b) shows micrograph of same specimen with EDS spectra collected at three different locations. Three locations from which the EDS was secured are marked as 1, 2 and 3 in the micrographs. All three EDS spectra indicated presence of C-A-S-H with different Ca/Si ratios. For example, the Ca/Si ratio is higher at location 1 (0.8) as compared to location 2 (0.3). This gives an indication that C-A-S-H is at different levels of development at different locations, as expected.

Figure 6 (c) shows EDS spectra at a magnification level of 5,000 taken from a different location. A flower-like structure of calcium hydroxide crystals is evident, which indicates presence of un-reacted hydrated lime in the stabilized specimen. This is in agreement with the micrograph presented in Figure 5 (a) for the lime paste.

7.4 Carnasaw soil with 15% CFA

The SEM micrographs of Carnasaw soil stabilized with 15% CFA are presented in Figures 7 (a) through (d). Figure 7 (a) reveals the formation of cementing products, with lamellar form, adjacent to the fly ash particles. The EDS analysis showed presence of Ca and Si indicating presence of C-S-H, the main cementing product responsible for strength gain (Choquette et al., 1987; Lav and Lav, 2000). The Ca/Si ratio of C-S-H phases identified in the CFA-stabilized soil was qualitatively determined to be approximately 3. Also, two additional peaks of Au and Pd appeared because specimens were sputter coated with alloy of gold-palladium. In viewing these samples, one would notice that the spherical particles of fly ash are joined strongly to the clay particles in its surrounding (Chang, 1995). It was also apparent that the fly ash particles served as nucleation sites for the growth of the hydration products (or coatings), as shown in Figure 7 (b). Formation of ettringite, $Ca_6[Al(OH)_6]_2.(SO_4)_3.26H_2O$, was also observed in the form of heaps of rod-like crystals (Figure 7 c). This observation was further confirmed by conducting EDS analysis, which suggested presence of Ca, Al and S with traces of Si and Ti as impurities. No areas were found showing normal ettringite spectra without traces of Si and Ti. Similar structure, as shown in Figure 2.25 (c), was reported as ettringite by other researchers (e.g., Mitchell and Dermatas, 1992; Intharasombat, 2003).

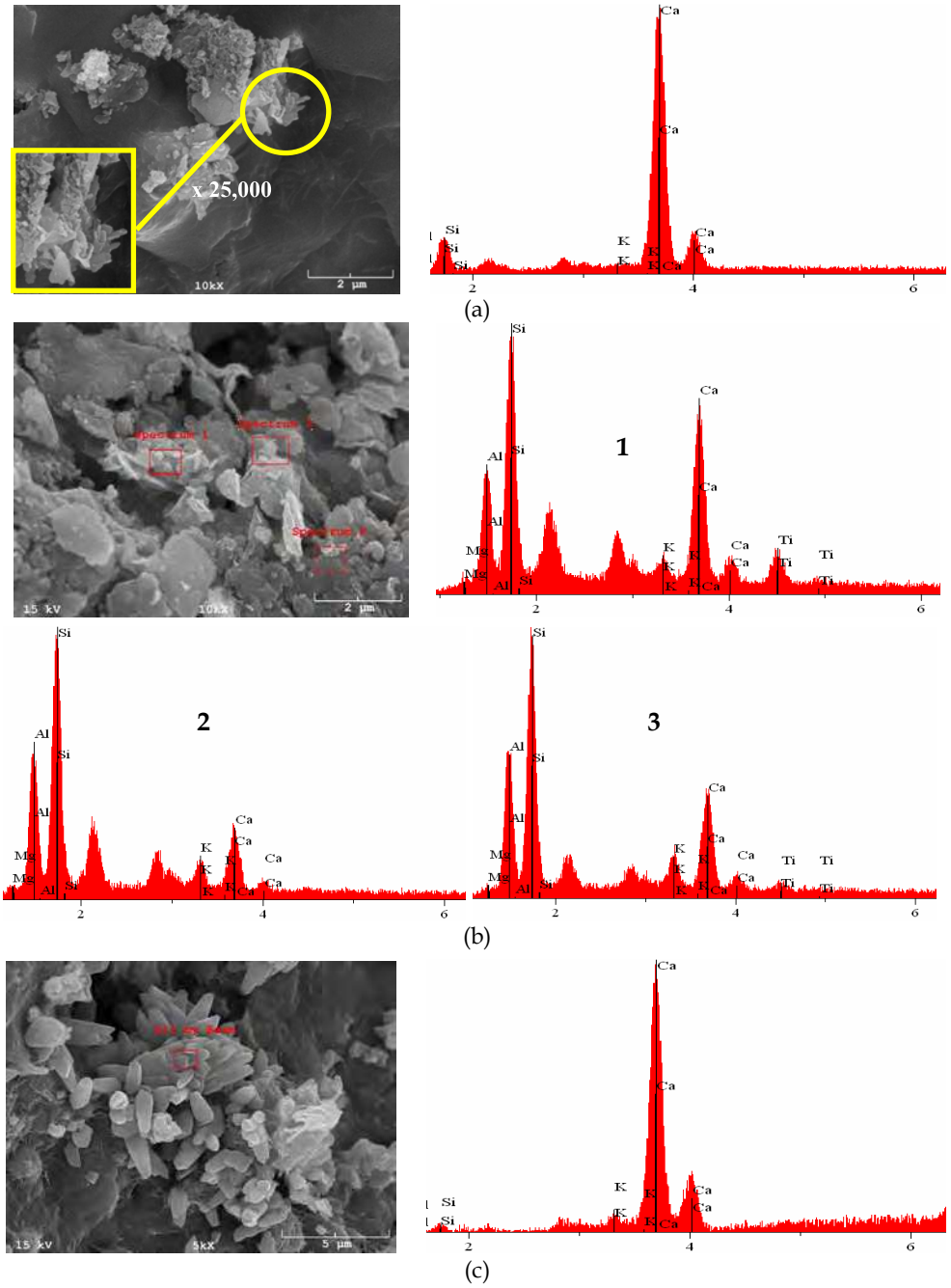

Fig. 6. SEM/EDS of 28-Day Cured 9% Lime-Stabilized Caranasaw Soil Specimens (a) C-S-H, (b) C-A-S-H, and (c) CH

Further, the SEM micrographs revealed that most of the fly ash particles were covered with a reaction shell as seen in Figure 7 (d). The approximate chemical composition of the outer shell was determined at location 1 and 3 by the EDS analysis and a typical composition is presented in pattern marked as point and 1 and 3. The composition of the shell was slightly different from that of the un-reacted inner fly ash surface which is shown in spectrum 2. The higher Ca peak in 1 and 3 compared to spectrum 2 suggests the initiation of reaction products (e.g., C-A-S-H) formation on the surface of fly ash particle. It should be noted that the exact quantitative composition cannot be obtained using the EDS analysis of the stabilized specimens.

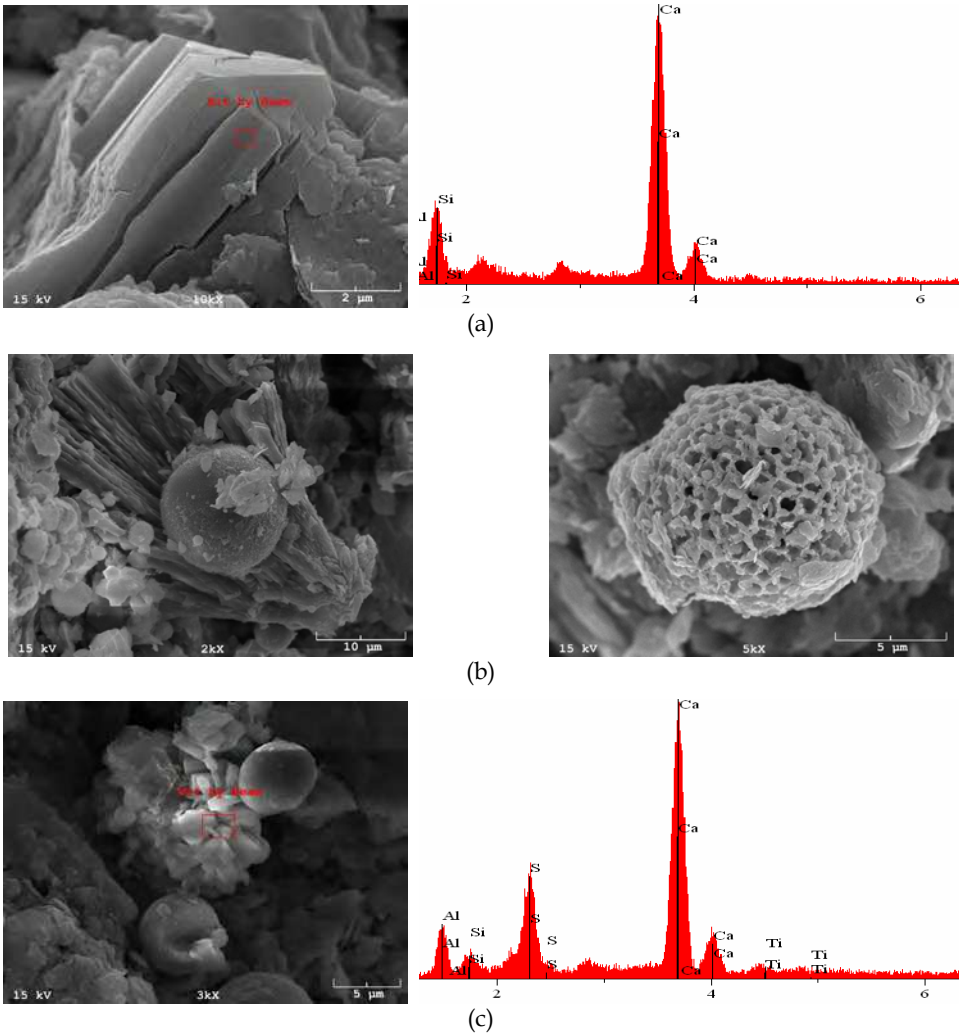

Fig. 7. SEM/EDS of 28-Day Cured 15% CFA-Stabilized Caranasaw Soil Specimens (a) C-S-H, (b) hydration coatings, and (c) ettringite crystal

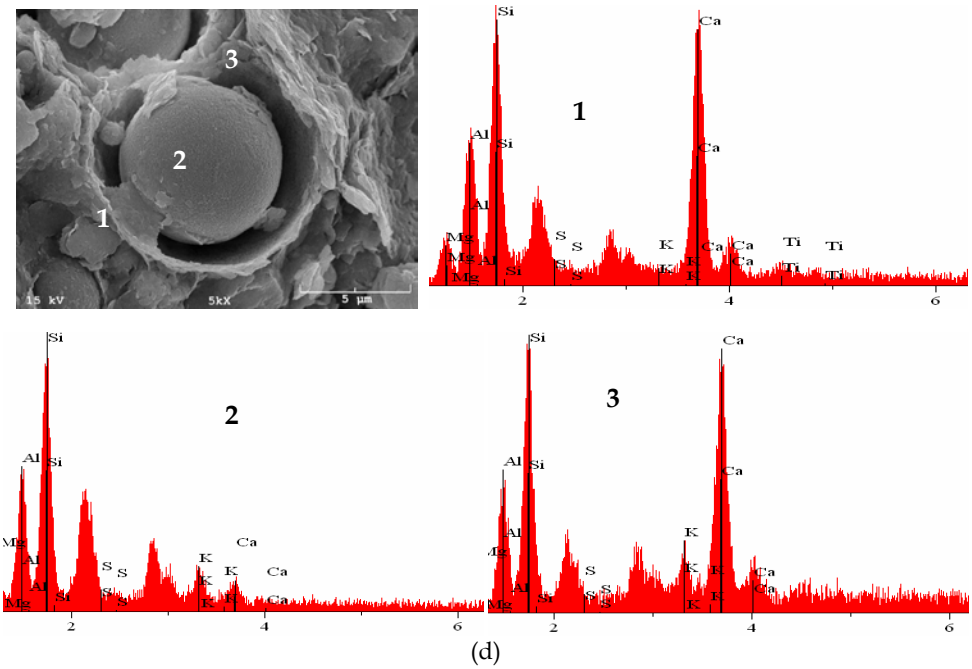

(d)

Fig. 7. (Cont'd). SEM/EDS of 28-Day Cured 15% CFA-Stabilized Caranasaw Soil Specimens (d) reaction shell of CFA particle

8.5 Carnasaw soil with 15% CKD

The SEM micrographs, as illustrated in Figures 8 (a) through (e) show significant changes in the microstructure of raw soil when mixed with CKD and cured for 28 days. It could be observed that flat clay structure surface observed in Figure 4 (a) is covered with cementitious reaction products, as shown in Figure 8 (a). Figure 8 (a) shows the C-A-S-H ($xCaO.yAl_2O_3.zSiO_2.wH_2O$) phase development which contains distinct peaks of Ca, Si and Al elements based on the EDS analysis, consistent with observation reported by Chaunsali and Peethamparan (2010). The Ca/Si ratio of approximately 3 is also evident from Figure 8 (a). The SEM micrograph at a different location revealed presence of C-S-H phase with Ca/Si ratio less than 1 (Figure 8 (b)). Additionally, C-S-H phases with very high Ca/Si ratio (>10) are also evident from the SEM micrograph and EDS spectra taken at different locations (Figure 8 (c)).

Figure 8 (d) shows micrographs of rose-shaped and web-shaped hydration coatings and bonds developed in 15% CKD-stabilized Carnasaw soil. Another prominent feature of the microstructure of 15% CKD-stabilized soil was the presence of needle-shaped ettringite crystals (Figure 8 (e)). The presence of ettringite crystals in CKD-stabilized soil is consistent with the observations reported by Peethamparan et al. (2008), Moon et al. (2009), and Chaunsali and Peethamparan (2011). Hence, improved modulus of elasticity exhibited by CKD-stabilized soil specimens after curing could be attributed to aforementioned reaction products.

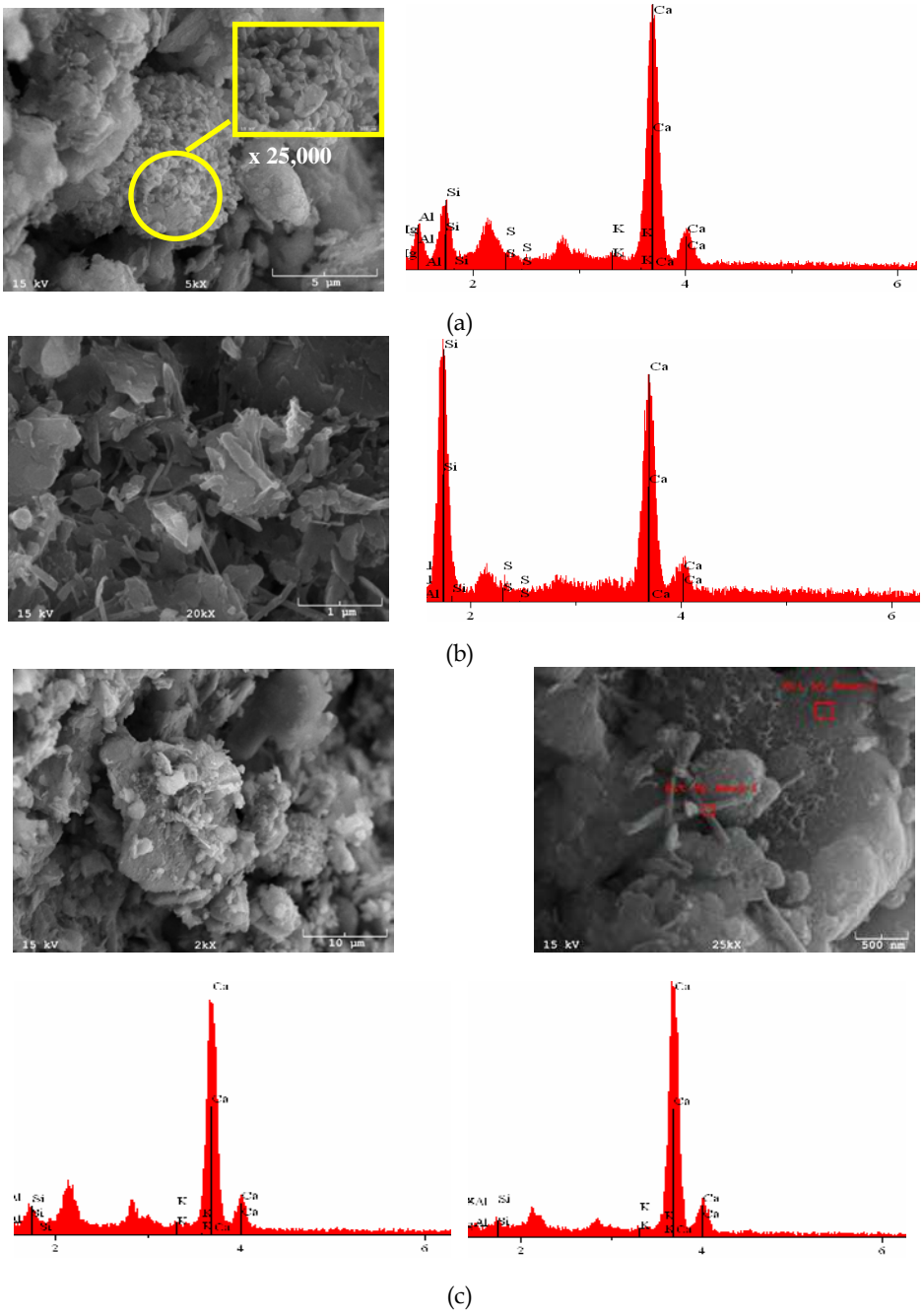

Fig. 8. SEM/EDS of 28-Day Cured 15% CKD-Stabilized Caranasaw Soil Specimens (a) C-A-S-H, (b) C-S-H, and (c) C-S-H

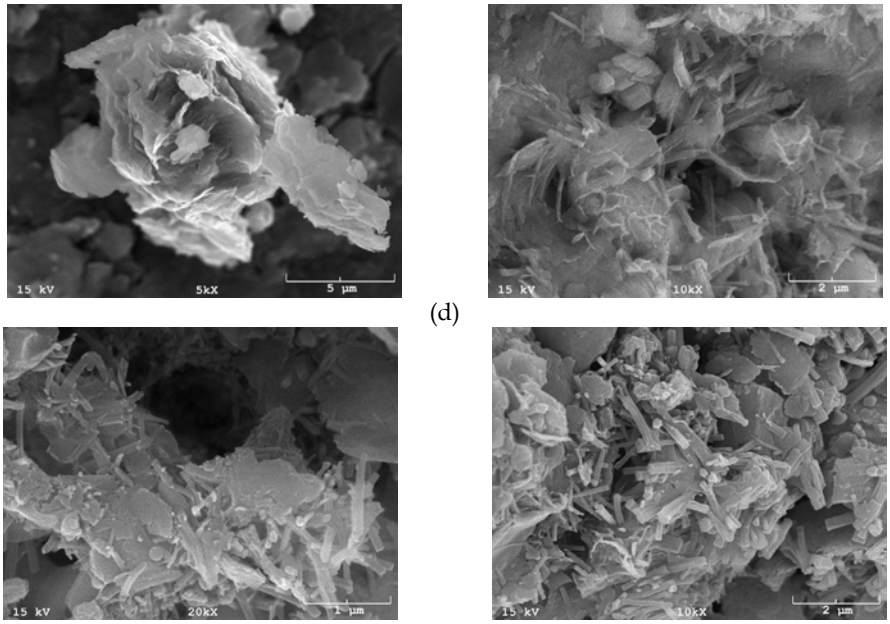

Fig. 8. (Cont'd). SEM/EDS of 28-Day Cured 15% CKD-Stabilized Caranasaw Soil Specimens (d) hydration coatings, and (e) ettringite crystals

9. XRD results

The XRD patterns of the raw soil and additives powder is presented in Figure 9. The raw soil showed presence of clay minerals namely, illite, $(K,H_3O)(Al,Mg,Fe)_2(Si,Al)_4O_{10}[(OH)_2,(H_2O)]$ and kaolinite $(Al_2Si_2O_5(OH)_4)$ which are expected in a fat clay with a PI value of 29. The presence of elements (Si, Al, Na, Fe, K) in aforementioned minerals of raw soil is also in agreement with elements observed from, EDS spectrum (Figure 4 (a)). The XRD pattern of raw lime powder indicates only presence of calcite $(CaCO_3)$ and calcium hydroxide $(Ca(OH)_2)$. The diffractogram of CFA powder revealed presence of three minerals namely, quartz (SiO_2), mullite $(Al_6Si_2O_{13})$, and merwinite $(Ca_3Mg(SiO_4)_2)$. This is in agreement with XRF results presented in Table 1. Similar minerals were reported by other researchers for class C fly ash (e.g., McCarthy, 2000; Chaunsali and Peethamparan, 2010). The CKD diffractogram showed presence of calcite, quick lime (CaO), quartz, and anhydrite $(CaSO_4)$. Similar observations were reported by Chaunsali and Peethamparan (2010).

The XRD patterns of raw and stabilized specimens are presented in one figure for comparison purpose (Figure 10). In general, there was a reduction in the peak intensity of most of the stabilized specimens, as can be seen by the reduction in peak heights of some of the peaks, particularly for the samples stabilized with 9% lime. This could be attributed to cementitious reactions between additive and clay minerals resulting in the reduction of the clay mineral intensities. Similar behavior was reported by Al-Rawas (2002). None of the peaks of the raw soil disappeared due to stabilization. It was noted that with the addition of 15% CFA, the peaks shifted away to the right from their original positions while

maintaining the same patterns. This could be due to instrument distortion during the XRD scanning process or conditions of the sample. The XRD pattern of CKD-stabilized specimens revealed additional peaks of calcite formed due to cementitious reactions.

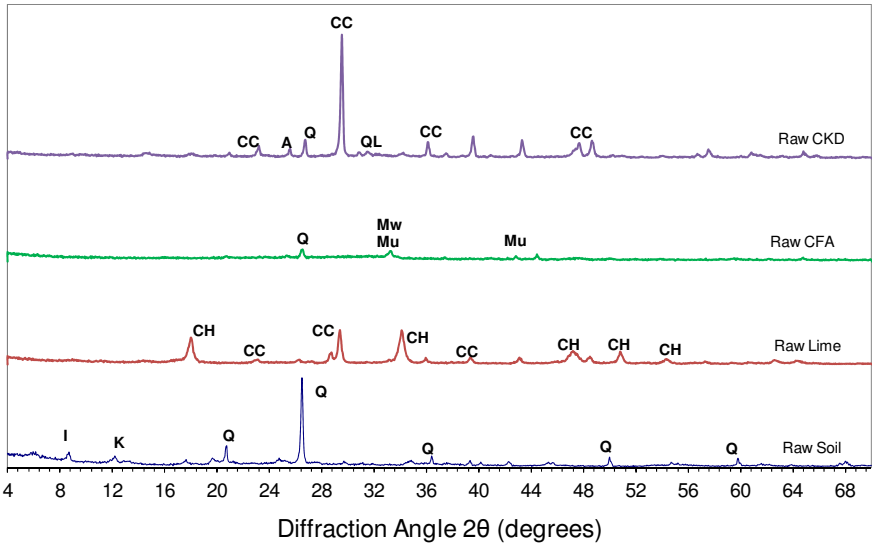

Fig. 9. XRD pattern for raw soil, lime, CFA and CKD powders [CC-calcite ($CaCO_3$), A-anhydrite ($CaSO_4$), QL-quicklime (CaO), Q-quartz (SiO_2), Mu-mullite ($Al_6Si_2O_{13}$), Mw-merwinite ($Ca_3Mg(SiO_4)_2$), CH-calcium hydroxide ($Ca(OH)_2$), I-illite, K-kaolinite)

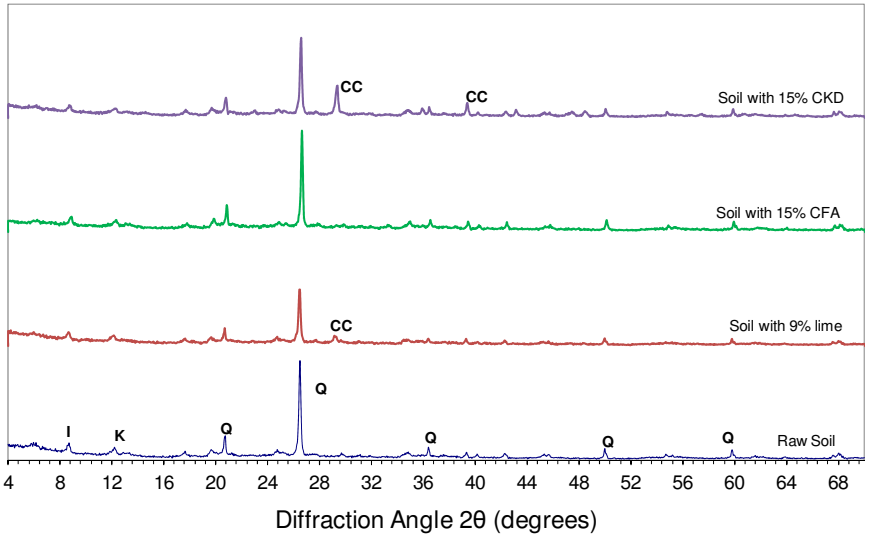

Fig. 10. XRD pattern for 9% lime-, 15% CFA- and 15% CKD-stabilized specimens [CC-calcite ($CaCO_3$), Q-quartz (SiO_2), I-illite, K-kaolinite)

10. Conclusions

Based on the study presented, in this chapter the following conclusions can be derived:

1. The results from pH tests showed that 5% lime provide an asymptotic behavior (less than 1% increase in pH w.r.t raw soil pH) in Carnasaw soil-lime mixtures. No such asymptotic behavior was observed for Carnasaw soil stabilized with CFA and CKD.
2. All three additives improved the modulus of elasticity values of Carnasaw soil (fat clay) specimens; however, degree of improvement varied with the type of additive.
3. The normalized modulus of elasticity values is better correlated with additive properties – free-lime content, alkali content, loss on ignition, percent passing No. 325 sieve, specific surface area, and pH.
4. In general, microscopic analyzes confirm that the addition of lime or CFA or CKD to soil induces beneficial reactions and significant improvements in stiffness. Also, it could be concluded that the formation of reaction products such as C-S-H, C-A-S-H and ettringite contributed to strength development of stabilized soil.
5. The lime-stabilized specimens indicated presence of both C-S-H and C-A-S-H phases in addition to unreacted calcium hydroxide. Additionally, C-A-S-H at different levels of development at different locations was identified.
6. The SEM and EDS results showed presence of C-S-H, C-A-S-H and ettringite crystals in both CFA-and CKD-stabilized specimens. The fly ash particles served as nucleation sites for the growth of the hydration products with reaction products initiating from the surface.
7. The Ca/Si ratio in C-S-H and C-A-S-H phases was found vary between 0.3 – 12 at different locations of the stabilized specimen. The presence of higher Ca/Si ratio phases in the microstructure of the stabilized specimen could be due to possible secondary cementitious reactions between soil and Ca^{2+} ion of additive.
8. The XRD results showed a general reduction in all clay minerals' peak intensities particularly in the case of lime-stabilized samples. However, none of the peaks of the raw soil disappeared due to stabilization.

11. Acknowledgment

The authors are thankful to the Oklahoma Department of Transportation (ODOT) and Oklahoma Transportation Center (OTC) for providing funds for this project. Technical assistance from Dr. Preston Larson (University of Oklahoma) and Tim Rawlsky (Lafarge North America) is gratefully acknowledged.

12. References

Air Force Manual (AFJMAN) (1994). "Soil Stabilization for Pavements," *Technical Manual No. 5-822-14*, Departments of the Army and Air Force, Washington, DC.

Al-Rawas, A. A. (2002). Microfabric and mineralogical studies on the stabilization of an expansive soil using cement by-pass dust and some types of slags. *Canadian Geotechnical Journal*, Vol. 39, Issue 5, pp. 1150-1167

Al-Rawas, A. A., Taha, R., Nelson, J. D., Al-Shab, T. B., and Al-Siyabi, H. (2002). "A Comparative Evaluation of Various Additives Used in the Stabilization of Expansive Soils," *ASTM Geotechnical Testing Journal*, Vol. 25, No. 2, pp. 199 – 209.

Baghdadi, Z. A., and Rahman, M. A. (1990). "The Potential of Cement Kiln Dust for the Stabilization of Dune Sand in Highway Construction," *Building and Environment*, Vol. 25, No. 4, pp. 285 – 289.

Bhatty, J. I., Bhattacharja, S., and Todres, H. A. (1996). "Use of Cement Kiln Dust in Stabilizing Clay Soils," Portland Cement Association, Skokie, IL.

Bin-Shafique, S., Edil, T., and Benson, C. (2004). "Incorporating a Fly Ash Stabilized Layer into Pavement Design Case Study," *Geotechnical Engineering*, Vol. 157, No. 4, pp. 239 – 249.

Camargo, F. F., Edil, T. B., and Benson, C. H. (2009). "Strength and Stiffness of Recycled Base Materials Blended with Fly Ash," *Transportation Research Board 88th Annual Meeting*, CD-ROM Publication, Transportation Research Board, Washington, DC.

Cerato, A. B., and Lutenegger, A. J. (2002). "Determination of surface are of fine-grained soils by the ethylene glycol monoethyl ether (EGME) method," *ASTM Geotechnical Testing Journal*, Vol. 25, No. 3, pp. 1 – 7.

Chang, D.T. (1995). "Resilient Properties and Microstructure of Modified Fly Ash-stabilized Fine Grained Soils." *Transportation Research Record: Journal of the Transportation Research Board*, Vol. 1486, pp. 88 – 96.

Chapman, H. D. (1965). "Cation Exchange Capacity," *Methods of Soil Analysis*, American Society of Soil Agronomy, C. A. Black et al., Eds., Madison, WI, pp. 891 – 901.

Chaunsali, P., and Peethamparan, S. (2010). "Microstructural and Mineralogical Characterization of Cement Kiln Dust Activated Fly Ash Binder," *Transportation Research Board 89th Annual Meeting*, CD-ROM Publication, National Research Council, Washington, DC.

Chaunsali, P., and Peethamparan, S. (2011). Evloution of Strength, Microstructure and Mineralogical Composition of a CKD-GGBFS Binder. *Cement and Concrete Research*. Vol. 41, pp. 197-208.

Choquette, M., Berube, M. –A., and Locat, J. (1987). "Mineralogical and Microtextural Changes Associated with Lime Stabilization of Marine Clays from Eastern Canada," *Applied Clay Science*, Vol. 2, pp. 215 – 232.

Collins, R. J., and Emery, J. J. (1983). "Kiln Dust/Fly Ash Systems for Highway Bases and Subbases," U.S. Department of Transportation – Department of Energy Report, FHWA/RD-82/167.

Consoli, N. C., Lopes, L. S., and Heineck, K. S. (2009). "Key Parameters for the Strength Control of Lime Stabilized Soils," *ASCE Journal of Materials in Civil Engineering*, Vol. 21, No. 5, pp. 210 – 216.

Diamond, S., and Kinter, E. B. (1964). "Mechanisms of Soil-Lime Stabilization," *Highway Research Record*, Vol. 92, pp. 83 – 96.

Eades, J. (1962). "Reactions of $Ca(OH)_2$ with Clay Minerals in Soil Stabilization," PhD Thesis, University of Illinois, Urbana, IL.

Evangelos, S. (2006). "A Solution to the Problem of Predicting the Suitability of Silty-Clayey Materials for Cement-Stabilization," *Geotechnical and Geological Engineering*, Vol. 24, No. 2, pp. 379 – 398.

Ferguson, G., and Levorson, S. M. (1999). "Soil and Pavement Base Stabilization with Self-Cementing Coal Fly Ash," Final Report for American Coal Ash Association, Alexandria, VA.

Ghosh, A., and Subbarao, C. (2001). "Microstructural Development in Fly Ash Modified with Lime and Gypsum," *ASCE Journal of Materials in Civil Engineering*, Vol. 13, No. 1, pp. 65 – 70.

Ghosh, A., and Subbarao, C. (2001). "Microstructural Development in Fly Ash Modified with Lime and Gypsum," *Journal of Materials in Civil Engineering*, Vol. 13, No. 1, pp. 65-70.

Gomez, J. D. P. (2009). "Influence of Curing Time on the Resilient Modulus of Chemically Stabilized Soils," MS Thesis, University of Oklahoma, Norman, OK.

Haston, J.S., and Wohlgemuth, S.K. (1985). "Experiences in the Selection of the Optimum Lime Content for Soil Stabilization." *Texas Civil Engineer*, November 1985, pp.17 – 20.

Horpibulsuk, S., Rachan, R., Chinkulkijniwat, A., Raksachon, Y., and Suddeepong, A. (2010).Analysis of Strength Development in Cement-stabilized Silty Clay from Microstructural Considerations, *Construction and Building Materials*, Vol. 24, pp. 2011-2021.

Hunter, D. (1988). "Lime-induced Heave in Sulfate-bearing Clay Soils," *Journal of Geotechnical Engineering*, Vol.114, No.2, pp.150 – 167.

Indian Road Congress (IRC) (2000). "State of the Art: Lime-Soil Stabilization," *Special Report*, IRC Highway Research Board, New Delhi, India.

Intharasombat, N. (2003). "Ettringite Formation in Lime Treated Sulfate Soils: Verification by Mineralogical and Swell Testing," MS Thesis, University of Texas, Arlington, TX

Jade (1999). *Materials Data Manual*, MDI, Livermore, CA, 94550.

Kavak, A., and Akyarh, A. (2007). "A field Application for Lime Stabilization," *Environmental Geology*, Vol. 51, pp. 987 – 997.

Khoury, N. N. (2005). "Durability of Cementitiously Stabilized Aggregate Bases for Pavement Application," PhD Thesis, University of Oklahoma, Norman, OK.

Khoury, N., and Zaman, M. M. (2007). "Durability of Stabilized Base Courses Subjected to Wet-Dry Cycles," *International Journal of Pavement Engineering*, Vol. 8, No. 4, pp. 265 – 276.

Kim, D., and Siddiki, N. (2004). "Lime Kiln Dust and Lime – A Comparative Study in Indiana," *Transportation Research Board 83rd Annual Meeting*, CD-ROM Publication, Transportation Research Board, Washington, DC.

Kolias, S., Kasselouri-Rigopoulou, V., and Karahalios, A. (2005). *Cement & Concrete Composites,* Vol. 27, pp. 301-313.

Kota, P. B. V. S., Hazlett, D., and Perrin, L. (1996). "Sulfate-Bearing Soils: Problems with Calcium-based Additives," *Transportation Research Record: Journal of the Transportation Research Board*, Vol. 1546, pp. 62 – 69.

Lav, A. H., and Lav, M. A. (2000). "Microstructural Development of Stabilized Fly Ash as Pavement Base Material," *ASCE Journal of Materials in Civil Engineering*, Vol. 12, No. 2, pp. 157 – 163.

Li, L., Edil, T. B., and Benson, C. H. (2009). "Properties of Pavement Geomaterials Stabilized with Fly Ash," *Proceedings of 2009 World of Coal Ash Conference*, Lexington, KY.

Little, D. N. (2000). "Evaluation of Structural Properties of Lime Stabilized Soils and Aggregates," *Mixture Design and Testing Protocol for Lime Stabilized Soils*, Vol. 3, National Lime Association report, http://www.lime.org/SOIL3.PDF, Last Accessed: Jan., 2007.

Locat, J., Tremblay, H., and Leroueil, S. (1996). "Mechanical and Hydraulic Behavior of a Soft Inorganic Clay Treated with Lime," *Canadian Geotechnical Journal*, Vol. 33, pp. 654 – 669.

Mallela, J., Quintus, H. V., and Smith, K. L. (2004). "Consideration of Lime-Stabilized Layers in Mechanistic-Empirical Pavement Design," F*inal Report submitted to the National Lime Association*, Arlington, VA.

McCarthy, G. J. (2000). "Energy: By-Products of Coal Combustion in Power Plants," Chapter 23, *Industrial Applications of X-Ray Diffraction*, editors: Chung, F. H. and Smith, D. K., Marcel Dekker Inc., New York, NY.

McCoy, W. J., and Kriner, R. W. (1971). "Use of Waste Kiln Dust for Soil Consolidation," Lehigh Portland Cement Co., Allentown, PA.

McManis, K. L., and Arman, A. (1989). "Class C Fly Ash as a Full or Partial Replacement for Portland Cement or Lime," *Transportation Research Record: Journal of the Transportation Research Board*, Vol. 1219, pp. 68 – 61.

Miller, G.A. and Azad, S. (2000). "Influence of Soil Type on Stabilization with Cement Kiln Dust." *Construction and Building Materials*, Vol. 14, pp. 89 – 97.

Miller, G. A. and Zaman, M. (2000). "Field and Laboratory Evaluation of Cement Kiln Dust as a Soil Stabilizer," *Transportation Research Record: Journal of the Transportation Research Board*, Vol. 1714, pp. 25 – 32.

Misra, A. (1998). "Stabilization Characteristics of Clays Using Class C Fly Ash," *Transportation Research Record: Journal of the Transportation Research Board*, Vol. 1611, pp. 46 – 54.

Mitchell, J. K., and Dermatas, D. (1990). "Clay Soil Heave Caused by Lime-Sulfate Reactions," *ASTM Special Technical Publication*, Vol. 1135, pp. 41 – 64.

Mitchell, J. K., and Dermatas, D. (1992). "Clay Soil Heave Caused by Lime-Sulfate Reactions," *ASTM STP 1135: Innovations and Uses for Lime*, Philadelphia, PA.

Mitchell, J.K. (1993). *Fundamentals of Soil Behavior*. 2nd Edition. John Wiley & Sons, NY.

Mohamed, A. M. O. (2002). "Hydro-mechanical Evaluation of Soil Stabilized with Cement-Kiln Dust in Arid Lands," *Engineering Geology*, Vol. 42, No. 8, pp. 901 – 921.

Moon, D. H., Grubb, D. G., and Reilly, T. L. (2009). "Stabilization/Solidification of Selenium-Impacted Soils Using Portland Cement and Cement Kiln Dust," *Journal of Hazardous Materials*, Vol. 168, pp. 944 – 951.

Nalbantoglu, Z. (2004). "Effectiveness of Class C Fly Ash as an Expansive Soil Stabilizer," *Construction and Building Materials*, Vol. 18, pp. 377 – 381.

Nalbantoglu, Z. (2006). "Lime Stabilization of Expansive Clay," *Expansive Soils,* Part 7, Vol. 1, pp. 341 – 348.

Nalbantoglu, Z. and Tuncer, E. R. (2001). "Compressibility and Hydraulic Conductivity of a Chemically Treated Expansive Clay," *Canadian Geotechnical Journal*, Vol. 38, pp. 154 – 160.

National Cooperative Highway Research Report (NCHRP) (1976). "Lime-Fly Ash-Stabilized Bases and Subbases," Transportation Research Board, National Council, Washington, DC.

ODOT (Oklahoma Department of Transportation) (2006). OHD L-49: Method of Test for Determining Soluble Sulfate Content in Soil, *Oklahoma Highway Department Test Method*, Oklahoma City, Oklahoma.

Parsons, R.L. and E. Kneebone. (2004). "Use of Cement Kiln Dust for the Stabilization of Soils," *Proceedings of Geo-Trans 2004*, Los Angeles, California, No. 1, pp. 1124 – 1131.

Parsons, R.L., Kneebone, E. and Milburn, J.P. (2004). "Use of Cement Kiln Dust for Subgrade Stabilization." *Final Report No. KS-04-03*, Kansas Department of Transportation, Topeka, KS.

Peethamparan, S. and Olek, J. (2008). "Study of the Effectiveness of Cement Kiln Dusts in Stabilizing Na-montmorillonite Clays," *ASCE Journal of Materials in Civil Engineering*,Vol. 20 No.2, pp.137 – 146.

Peethamparan, S., Olek, J. and Diamond, S. (2008). "Physicochemical Behavior of Cement Kiln Dust-Treated Kaolinite Clay," *Transportation Research Record: Journal of the Transportation Research Board*, Vol. 2059, pp. 80 – 88.

Petry, T. M., and Little, D. N. (1992). "Update on Sulfate Induced Heave in Treated Clays: Problematic Sulfate Levels," *Transportation Research Record: Journal of the Transportation Research Board*, Vol. 1362, pp. 51 – 55.

Phanikumar, B. R., and Sharma, R. S. (2004). "Effect of Fly Ash on Engineering Properties of Expansive Soils," *ASCE Journal of Geotechnical and Geoenvironmental Engineering*, Vol. 130, No. 7, pp. 764 – 767.

Prusinski, J. R., and Bhattacharia, S. (1999). "Effectiveness of Portland cement and lime in stabilizing clay soils," *Transportation Research Record: Journal of the Transportation Research Board*, Vol. 1632, pp. 215 – 227.

Puppala, A. J., E. Wattanasanticharoen, and A. Porbaha. (2006). "Expansive soils: Recent advances in characterization and treatment, A. Combined lime and polypropylene fiber stabilization for modification of expansive soils," Chapter 24, Taylor and Francis, NY.

Puppala, A. J., Griffin, J. A., Hoyos, L. R. and Chomtid, S. (2004). "Studies of Sulfate-Resistant Cement Stabilization Methods to Address Sulfate-Induced Soil Heave," *ASCE Journal of Geotechnical and GeoEnvironmental Engineering*, Vol.130, No.4, pp.391 – 402.

Puppala, A. J., Viyanant, C., Kruzic, A., and Perrin, L. (2002). "Evaluation of a modified sulfate determination method for cohesive soils," *Geotechnical Testing Journal*, Vol. 25, No. 1, pp. 85 – 94.

Puppala, A. J., Wattanasanticharoen, E., Intharasombat, N., and Hoyos, L. R. (2003). "Studies to Understand Soil Compositional and Environmental Variables on Sulfate Heave Problems," *Proceedings of Soil Rock America: 12th Pan American Conference on Soil Mechanics and Geotechnical Engineering*, Boston, MA.

Qubain, B. S., Seksinsky, E. J., and Li, J. (2000). "Incorporating Subgrade Lime Stabilization into Pavement Design," *Transportation Research Record: Journal of the Transportation Research Board*, Vol. 1721, pp. 3 – 8.

Rajasekaran, G., Murali, K., & Srinivasaraghavan, R. (1995). Fabric and mineralogical studies on lime treated marine clays. *Ocean Engng*, 24(3), 227-234.

Rajendran, D., and Lytton, R. L. (1997). "Reduction of Sulfate Swell in Expansive clay Subgrades in the Dallas district," *Texas Transportation Institute Report No. TX-98/3929-1*, Bryan, TX

Rao, S. M., and Shivananda, P. (2005). "Impact of Sulfate Contamination on Swelling Behavior of Lime-Stabilized Clays," *Journal of ASTM International,* Vol. 2, No. 6, pp. 1-10

Rollings, R. S., Burkes, J. P., and Rollings, M. P. (1999). "Sulfate Attack on Cement-stabilized Sand," *ASCE Journal of Geotechnical and Geoenvironmental Engineering*, Vol. 125, No. 5, pp. 364–372.

Sayah, A. I. (1993). "Stabilization of a Highly Expansive Clay Using Cement Kiln Dust," MS Thesis, University of Oklahoma, Norman, OK.

Sear, L.K.A. (2001). *Properties and Use of Coal Fly Ash – A Valuable Industrial By-Product*, Thomas Telford, Reston, VA.

Sezer, A., Inan, G., Yilmaz, R. and Ramyar, K. (2006). "Utilization of a Very High Lime Fly Ash for Improvement of Lzmir Clay," *Building and Environment*, Vol. 41, No. 2, pp. 150 – 155.

Sreekrishnavilasam, A., Rahardja, S., Kmetz, R. and Santagata, M. (2007). "Soil Treatment Using Fresh and Landfilled Cement Kiln Dust," *Construction and Building Materials*, Vol. 21, pp. 318 – 327.

Stutzman, P. (2004). "Scanning Electron Microscopy Imaging of Hydraulic Cement Microstructure," *Cement and Concrete Research*, Vol. 26, pp. 957-966.

Zaman, M., Laguros, J. G., and Sayah, A. I. (1992). "Soil Stabilization using Cement Kiln Dust," *Proceeding of the 7th International Conference on Expansive Soils*, Dallas, TX, pp. 1 – 5.

Zaman, M., Laguros, J., Tian, P., Zhu, J, and Pandey, K. (1998). "Resilient Moduli of Raw and Stabilized Aggregate Bases and Evaluations of Layer Coefficients for AASHTO Flexible Pavement Design." *ORA 125-4262*, Item 2199, Department of Transportation, Oklahoma City, OK.

Zheng, J. and Qin, W. (2003). "Performance Characteristics of Soil-Cement from Industry Waste Binder," *ASCE Journal of Materials in Civil Engineering*, Vol. 15, No. 6, pp. 616 – 618.

Zia, N., and Fox, P. J. (2000). "Engineering Properties of Loess-Fly Ash Mixtures for Roadbase Construction," *Transportation Research Record: Journal of the Transportation Research Board*, Vol. 1714, pp. 49 – 56.

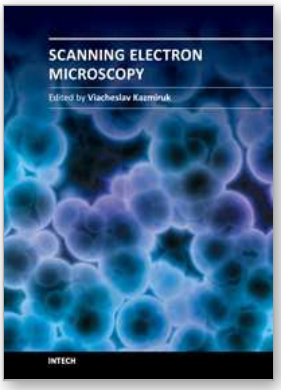

Scanning Electron Microscopy
Edited by Dr. Viacheslav Kazmiruk

ISBN 978-953-51-0092-8
Hard cover, 830 pages
Publisher InTech
Published online 09, March, 2012
Published in print edition March, 2012

Today, an individual would be hard-pressed to find any science field that does not employ methods and instruments based on the use of fine focused electron and ion beams. Well instrumented and supplemented with advanced methods and techniques, SEMs provide possibilities not only of surface imaging but quantitative measurement of object topologies, local electrophysical characteristics of semiconductor structures and performing elemental analysis. Moreover, a fine focused e-beam is widely used for the creation of micro and nanostructures. The book's approach covers both theoretical and practical issues related to scanning electron microscopy. The book has 41 chapters, divided into six sections: Instrumentation, Methodology, Biology, Medicine, Material Science, Nanostructured Materials for Electronic Industry, Thin Films, Membranes, Ceramic, Geoscience, and Mineralogy. Each chapter, written by different authors, is a complete work which presupposes that readers have some background knowledge on the subject.

How to reference
In order to correctly reference this scholarly work, feel free to copy and paste the following:

Pranshoo Solanki and Musharraf Zaman (2012). Microstructural and Mineralogical Characterization of Clay Stabilized Using Calcium-Based Stabilizers, Scanning Electron Microscopy, Dr. Viacheslav Kazmiruk (Ed.), ISBN: 978-953-51-0092-8, InTech, Available from: http://www.intechopen.com/books/scanning-electron-microscopy/microstructural-and-mineralogical-characterization-of-clay-stabilized-using-calcium-based-stabilizer

INTECH
open science | open minds

InTech Europe
University Campus STeP Ri
Slavka Krautzeka 83/A
51000 Rijeka, Croatia
Phone: +385 (51) 770 447
Fax: +385 (51) 686 166
www.intechopen.com

InTech China
Unit 405, Office Block, Hotel Equatorial Shanghai
No.65, Yan An Road (West), Shanghai, 200040, China
中国上海市延安西路65号上海国际贵都大饭店办公楼405单元
Phone: +86-21-62489820
Fax: +86-21-62489821